Influence of Different Annealing Temperatures on the Structural and Optical Properties of TiO_2 Nanoparticles Synthesized via Sol-Gel Method: Potential Application as UV Sensor

Nur Munirah Safiay[1,2*], Rozina Abdul Rani[3], Najwa Ezira Ahmed Azhar[1,4], Zuraida Khusaimi[1,2], Fazlena Hamzah[5], and Mohamad Rusop[1,4]

[1]*NANO-SciTech Centre (NST), Institute of Science (IOS), Universiti Teknologi MARA (UiTM), 40450 Shah Alam, Selangor, Malaysia*

[2]*Faculty of Applied Sciences, Universiti Teknologi MARA (UiTM), 40450 Shah Alam, Selangor, Malaysia*

[3]*Faculty of Mechanical Engineering, Universiti Teknologi MARA (UiTM), 40450 Shah Alam, Selangor, Malaysia*

[4]*NANO-ElecTronic Centre (NET), Faculty of Electrical Engineering, Universiti Teknologi MARA (UiTM), 40450 Shah Alam, Selangor, Malaysia*

[5]*Faculty of Chemical Engineering, Universiti Teknologi MARA (UiTM), 40450 Shah Alam, Selangor, Malaysia*

**** Corresponding author:***

tel: +603-55444412
email: munirahsafiay@gmail.com

Received: December 6, 2019
Accepted: June 26, 2020

DOI: 10.22146/ijc.52255

Abstract: *In this research, TiO_2 thin films were prepared using a simple sol-gel spin coating process. The films were characterized using Field Emission Scanning Electron Microscopy (FE-SEM), Energy Dispersive Ray (EDX), X-ray diffraction (XRD) and Ultraviolet–visible Spectrophotometer in order to investigate the influence of different annealing temperatures to the structural and optical properties of TiO_2. The surface morphology images from FE-SEM display a uniform layer of nanoparticles with a sample of 500 °C possess the most uniform and the visible spherical grain of TiO_2 nanoparticles. EDX spectra confirm the presence of Ti and O elements in the samples. The structural properties from the XRD pattern demonstrate that the films are crystalline at a temperature of 500 and 600 °C and the peak (101) intensity was increased as the annealing temperature increased. They exist in the anatase phase at the preferred plane orientation of (101). The calculated crystallite size for 500 and 600 °C samples is 19.22 and 28.37 nm, respectively. The films also possessed excellent absorption in the ultraviolet (UV) region with optical band gap energy ranging from 3.32 to 3.43 eV. These results can be fundamental for the fabrication of a UV sensing device.*

Keywords: *TiO_2; annealing; optical; UV; absorption*

■ INTRODUCTION

Titanium dioxide (TiO_2) or titania is an n-type semiconductor that existed in three different phases: brookite, anatase, and rutile [1-3]. TiO_2 has gained wide attention due to chemical stability, chemical inertness, non-toxicity, biocompatibility and low cost [4-5]. TiO_2 can be synthesized via the sol-gel method, electrodeposition, hydrothermal, sputtering, Chemical Vapor Deposition (CVD) and the host of others to produce a different type of nanostructures [6-7]. Among all of the methods, sol-gel synthesis is one of the most preferable methods in synthesizing TiO_2 because it is facile, low cost and easy to control and producing good quality of thin films [8]. Sol-gel spin coating method also provided low temperature synthesis method compared to high temperature synthesis method such as CVD. Hence, this process is more energy saving and environmentally friendly. In producing highly crystalline thin films, treatment is needed. The common treatment method was annealing treatment. Annealing of TiO_2 thin films not only improved the crystallinity but

also the surface morphology. The purpose of annealing also to transform the amorphous structure of the film to a more crystalline structure [9]. It was also reported elsewhere that annealing makes the grain size becomes larger and the surface becomes rougher [9-10].

In this experiment, we discuss the effect of annealing temperature on the structural and optical properties of TiO_2 thin film. Previously, a few types of research suggested an optimum temperature of 450 °C for annealing but in this work, we further optimized the annealing temperature for the fabrication of UV sensor. In the fabrication of the UV sensor, the criteria of the synthesized TiO_2 films needed are high absorptivity in the UV region and have an optical band gap of > 3.00 eV.

■ EXPERIMENTAL SECTION

Materials

Titanium isopropoxide ($Ti(OCH(CH_3)_2)_4$; 97% purity; Aldrich), absolute ethanol (C_2H_5OH; 99.5% purity; Systerm), glacial acetic acid (CH_3COOH; 99.7% purity; J.T. Baker) and Triton X-100 ($C_{14}H_{22}O(C_2H_4O)_n$ (n = 9-10); 99.9% purity; Aldrich) and DI water.

Instrumentation

The effect of annealing temperatures on the surface morphology of TiO_2 thin films was observed by field emission scanning electron microscope (FESEM; JOEL JSM-7600F). The crystalline property was characterized by X-ray diffraction measurement (XRD; PANalytical X'Pert PRO). The film thickness was measured using a surface profilometer (KLA Tencor P-6). Elemental or compositional analysis was carried out by energy dispersive X-ray spectroscopy (EDX; INCA). The optical property was investigated using an ultraviolet-visible spectrophotometer (UV-Vis; Varian Cary 5000).

Procedures

Firstly, glass substrates (Duran Group) were cut into 1.5 cm × 2 cm in size by using a diamond cutter. Then, for the cleaning process of the glass substrates, they were immersed in a beaker containing acetone and placed in an ultrasonic water bath and sonicated for 10 min. Next, glass substrates were rinsed with deionized (DI) water and then were immersed in methanol and sonicated for another 10 min. After sonication with methanol, glass substrates were rinsed again with DI water and finally sonicated for another 10 min in a beaker filled with DI water. After the cleaning process, the substrates were blown with nitrogen gas and kept dry in sample containers before the deposition process. The preparation of TiO_2 solution was carried out using titanium isopropoxide, absolute ethanol, glacial acetic acid and Triton X-100 and DI water. Titanium isopropoxide was dissolved in absolute ethanol, which acts as a solvent under continuous stirring on a hot plate. 1.25 mL of glacial acetic acid, 0.09 mL of DI water and 0.01 mL of Triton X-100 was added to the solution as a surfactant and the solution was stirred for 2 h at ambient temperature. The solution was left aging for 24 h prior to the spin coating process. In the spin coating process, deposition speed was fixed at 3000 rpm and deposition time was in 50 sec. The deposition was repeated seven times and each layer was pre-heated at 150 °C for 10 min. Then, the thin films were annealed in a furnace at a different annealing temperature of as-grown, 400, 500 and 600 °C for 1 h.

■ RESULTS AND DISCUSSION

Structural Analysis

Fig. 1 depicts the XRD pattern of the synthesized films of TiO_2 annealed at different temperatures of 400, 500, and 600 °C respectively. The diffraction angles measured were from 10° to 70°. From the XRD pattern, TiO_2 thin films crystallized at a temperature of 500 and 600 °C. Both as-grown and 400 °C films were amorphous. The crystalline samples show the anatase phase (JCPDS 00-004-0477) with a tetragonal crystal structure. From the plots, the anatase phase was confirmed by peaks at 2θ = 25.2° and 48.7° corresponding to the (101) and (200) orientation planes, respectively [9]. The highest intensity of the diffraction peak at around ~25° shows a preferred oriented anatase polycrystalline structure for all of the samples. In addition, neither other titania phases, rutile nor brookite were detected in the samples, proving the purity of the anatase phase. The absence of a rutile peak also agrees with the previous report that the transformation of anatase to rutile begins at 1000 °C for

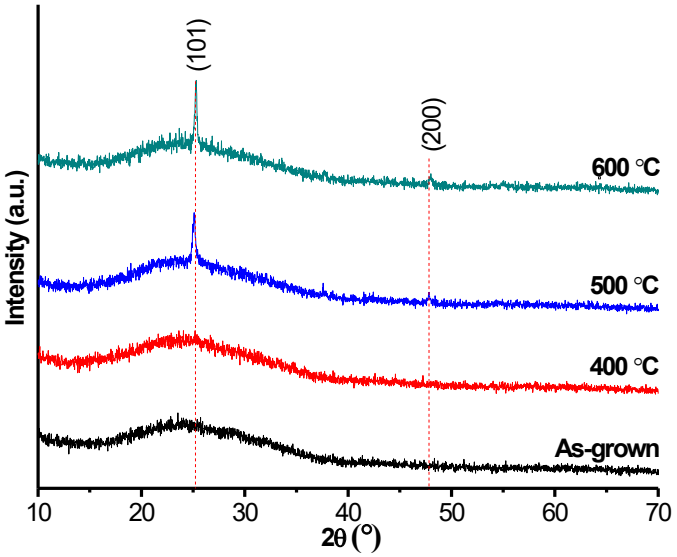

Fig 1. XRD pattern of TiO_2 thin films

sol-gel synthesis [11]. In addition, the crystallinity of the films also increased with increasing annealing temperature. This can be observed by the sharpness of peak intensity at preferred (101) peak. The more intense peaks revealed that the particle size increases at higher annealing temperatures [12].

From the XRD pattern, full-width-at-half-maximum (FWHM) of a peak intensity profile can be determined, which will be used in the Scherrer formula (Eq. (1)) to estimate the average crystallite size [13]:

$$D = \frac{0.94\lambda}{\beta\cos\theta} \quad (1)$$

where D is the crystallite size, λ is the wavelength of X-rays, β is the full width at half maximum of XRD peak and θ is the diffraction angle. The calculated crystallite sizes for 500 and 600 °C were 19.22 and 28.37 nm, respectively. The crystallite size increased when the annealing temperature increased. When the heat was applied to the TiO_2 films, the particles grew because the activation energy of TiO_2 nanoparticles was very minimal [12]. In addition, lattice spacing, lattice strain and dislocation density were also calculated by using Eq. (2), (3) and (4) [7].

$$d_{hkl} = \frac{\lambda}{2\sin\theta} \quad (2)$$

$$\varepsilon = \frac{\beta\cot\theta}{4} \quad (3)$$

$$\delta = \frac{1}{D^2} \quad (4)$$

Here, d_{hkl} is the lattice spacing, ε is the lattice strain, and δ is the dislocation density. The values were tabulated in Table 1. From Table 1, it can be seen that D values were increasing when the annealing temperature increased. This proved that the annealing temperature does play a role in tuning the crystal size [14]. This result also agrees with the previous reports regarding the annealing process which induces diffusion-driven phase segregation hence resulting in a non-homogenous composition and increasing crystal size [14]. The value of the lattice strain is positive (tensile strain). It is well known that the annealing treatment will reduce the tensile strain in thin films. Therefore, the further increase of annealing temperature, the tensile strain tends to change in the opposite direction of strain (compressive), indicating the more tense films [13]. When the lattice strain increase, the dislocation density is also increased.

Surface Morphology

The surface morphology of TiO_2 thin films was characterized by FE-SEM. Fig. 2 represents the surface morphology of all samples at a magnification of 80,000×. The amorphous as-grown film shows that no nanoparticles formed due to the no energy treatment applied to form nanoparticles. In nanotechnology, high energy treatment is needed in the formation of well crystalline nanoparticles. At 400 °C, the grain of nanoparticles was started to form but the spherical shape of nanoparticles still cannot be seen clearly and higher energy is needed to form better surface morphology. At 500 °C, the spherical shape of TiO_2 nanoparticles can be

Table 1. Values for crystallite size, lattice spacing, lattice strain, and dislocation density from XRD analysis

Sample (°C)	2θ at (101) plane (°)	$FWHM_{(101)}$ (°)	Crystallite size, D (nm)	d-spacing (Å)	Lattice Strain, ε (%)	Dislocation Density, δ (× 10^{-12} m^{-2})
500	25.09	0.442	19.22	0.182	0.236	2.71
600	25.26	0.230	28.37	0.180	0.159	1.24

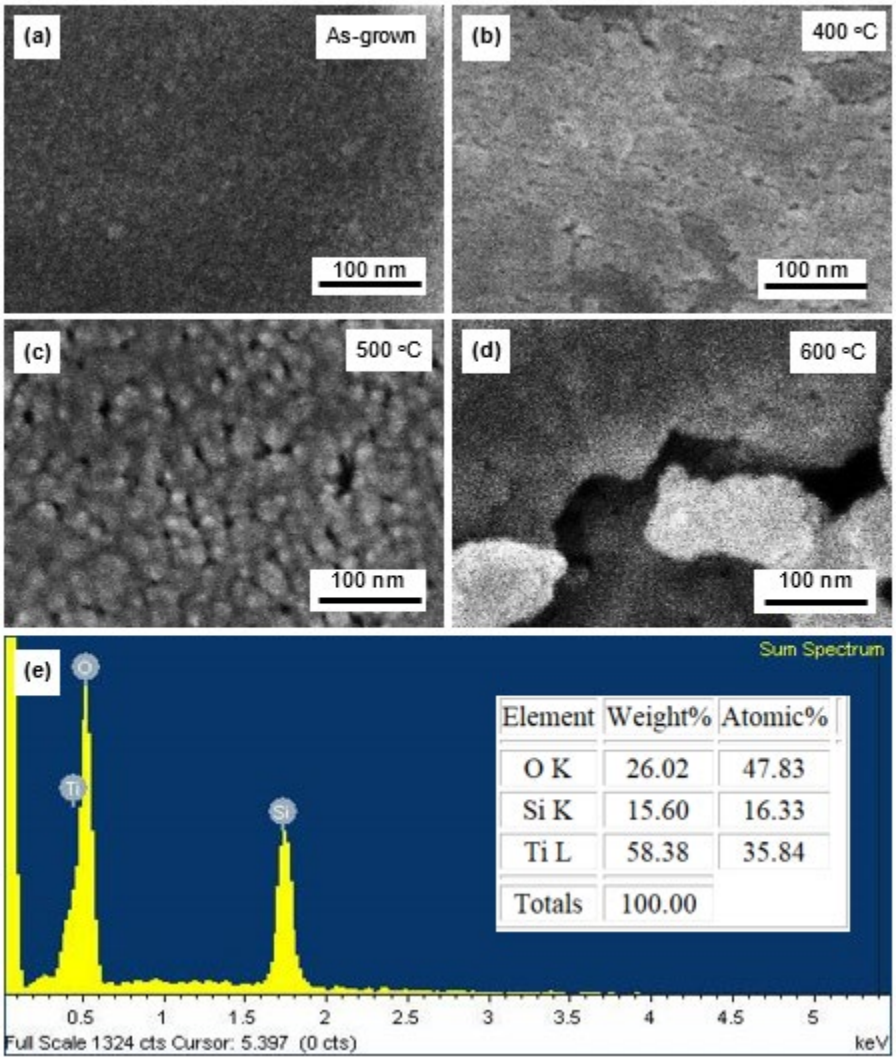

Fig 2. Surface morphology of TiO_2 thin films

observed clearly and the surface of the film was uniform and smooth. When sufficient heat was applied to the TiO_2 films, the particles grew because the activation energy of TiO_2 nanoparticles was very minimal [12]. However, at 600 °C, the film surfaces became rough and crumbled. A previous study reported that the glass substrate started to deform when the annealing temperature at about 600 °C, leading to the deterioration of the film [15].

The elemental analysis of the prepared thin films was examined by EDX as depicted in Fig. 2(e). The EDX result indicated that the TiO_2 sample was mainly composed of Ti and O elements which is consistent with the stoichiometric of TiO_2 [16]. The Ti elements were confirmed by the peak at Lα = 0.4522 keV where the electron from M orbital filled in the hole left by the kicked-out electron in L orbital. Meanwhile, O elements were confirmed by the peak at Kα = 0.5249 keV where the electron from L orbital filled in the hole left by the kicked-out electron in K orbital. The additional peaks associated with Si were due to the glass substrate. This EDX analysis assuring that there is no presence of other impurities in the film [17-18].

Optical Analysis

To further obtain information on the light-absorption properties of TiO_2 thin films, UV-Vis analysis was performed. UV–Vis transmittance spectra at room temperature for the samples in the wavelength range from approximately 300 nm to 800 nm illustrated

in Fig. 3. The transmittance spectrum can be divided into two regions i.e. ultra-violet region (< 390 nm) and visible light region (400–800 nm). All samples show average transparency in the visible region and absorbed in the UV range at a wavelength of 300 nm. The abrupt decrease in the transparency of all films in the UV region is due to the fundamental light absorption of TiO_2 [19].

The UV–Vis spectral data are used to obtain the absorption coefficient via Lambert's Law based on Eq. (5) as follows [20]:

$$\alpha = \frac{1}{t}\ln\frac{(1)}{T} \quad (5)$$

where t is the thickness of the film, and T is the transmittance of the film. The absorption coefficients of TiO_2 thin films were displayed in Fig. 4. The plotted graph shows that absorption edges can be observed in the UV region (< 400 nm) for all samples. All films exhibited high absorption of light at the UV region. The 500 °C film produced the best absorption at UV region due to the appearance of fine nanoparticles which magnify the surface area of the film and increase the optical scattering effect, hence exhibited excellent light absorption [21].

In addition, the band gap energies E_g of the synthesized and deposited samples are also calculated based on the Tauc's plot in the measured range using Eq. (6) as follows [20]:

$$(\alpha h\nu)^{1/2} = A(h\nu - E_g) \quad (6)$$

where α is the absorption coefficient, hν is the photon energy, A is an absorption constant, and E_g is the band gap.

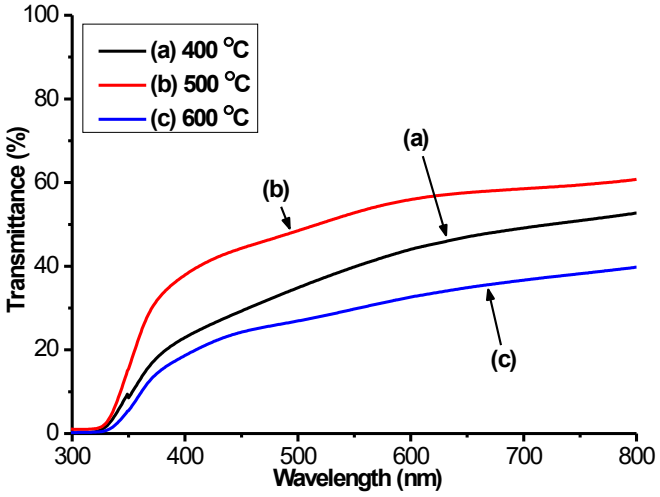

Fig 3. Transmittance spectra of TiO_2 thin films

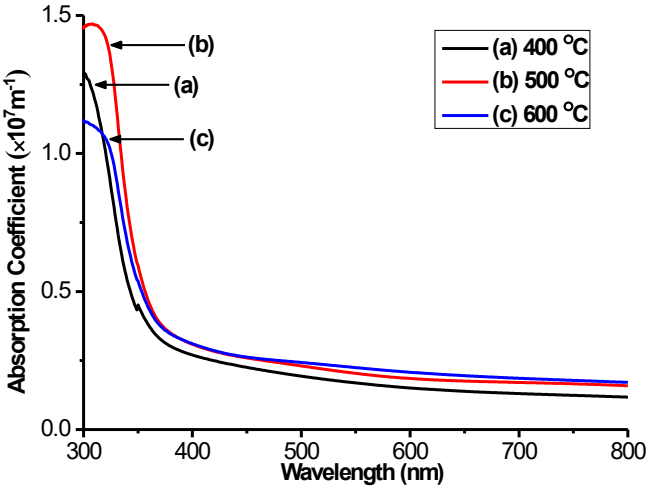

Fig 4. Absorption coefficient spectra of TiO_2 thin films

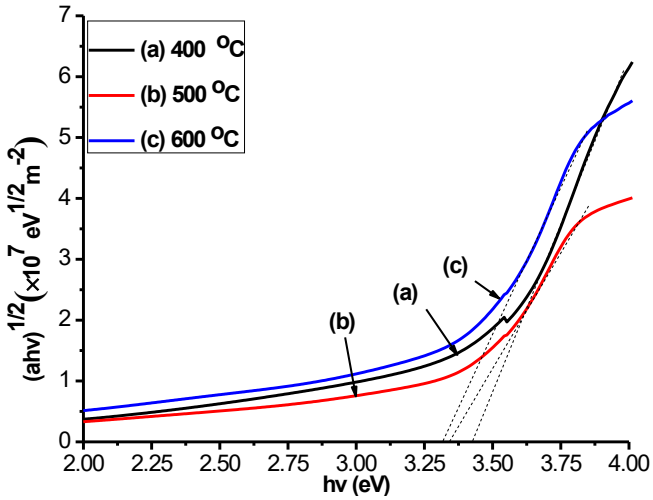

Fig 5. Tauc's plot of TiO_2 thin films

The band gap energy E_g was extrapolated from the linear line on the plotted graph in Fig. 5 of $(\alpha h\nu)^{1/2}$ versus the hν curve for the deposited samples. The band gap values obtained were 3.43, 3.35 and 3.32 eV for 400, 500 and 600 °C, respectively. There were no significant changes were observed in E_g.

■ CONCLUSION

In this work, we successfully synthesized TiO_2 thin films by conducting a simple and low-cost synthesis method using the sol-gel spin coating process. These nanoparticulate thin films were annealed in air at different annealing temperatures for 1 h. XRD pattern confirmed the films show good crystallinity and exist in the anatase phase at temperature 500 °C and above. The

calculated crystallite sizes for 500 and 600 °C were 19.22 and 28.37 nm, respectively. Though higher crystallite size is preferred, 500 °C was chosen as the optimized annealing temperature due to the analysis of other properties. The surface morphology of 500 °C films shows the clearest granular spherical shape of TiO_2 nanoparticles compared to other samples and EDX spectra confirmed the presence of titanium and oxygen elements in the samples. The absorption coefficient also shows 500 °C films to have the highest absorbance in the UV region with an optical band gap energy of 3.35 eV. These results indicate that TiO_2 thin film has a good potential for an optical-based device such as a UV sensor.

■ ACKNOWLEDGMENTS

This work is financially supported by FRGS grant 600-IRMI/FRGS 5/3 (081/2017), Institute of Research Management & Innovation (IRMI), Universiti Teknologi MARA (UiTM).

■ REFERENCES

[1] Ahmad, I., Usman, M., Zhao, T., Qayum, S., Mahmood, I., Mahmood, A., Diallo, A., Obayi, C., Ezema, F.I., and Maaza, M., 2018, Bandgap engineering of TiO_2 nanoparticles through MeV Cu ions irradiation, *Arabian J. Chem.*, 13 (1), 3344–3350.

[2] Blanco, E., González-Leal, J.M., and Ramírez-del Solar, M., 2015, Photocatalytic TiO_2 sol–gel thin films: Optical and morphological characterization, *Sol. Energy*, 122, 11–23.

[3] Zhang, X., Li, W., and Yang, Z., 2015, Toxicology of nanosized titanium dioxide: An update, *Arch. Toxicol.*, 89 (12), 2207–2217.

[4] Khan, M.M., Ansari, S.A., Pradhan, D., Ansari, M.O., Han, D.H., Lee, J., and Cho, M.H., 2014, Band gap engineered TiO_2 nanoparticles for visible light induced photoelectrochemical and photocatalytic studies, *J. Mater. Chem. A*, 2 (3), 637–644.

[5] Yazid, S.A., Rosli, Z.M., and Juoi, J.M., 2018, Effect of titanium (IV) isopropoxide molarity on the crystallinity and photocatalytic activity of titanium dioxide thin film deposited via green sol–gel route, *J. Mater. Res. Technol.*, 8 (1), 1434–1439.

[6] Lourduraj, S., and Williams, R.V., 2017, Effect of molarity on sol–gel routed nano TiO_2 thin films, *J. Adv. Dielectr.*, 7 (6), 1750–1757.

[7] Desai, N.D., Khot, K.V., Dongale, T., Musselman, K.P., and Bhosale, P.N., 2019, Development of dye sensitized TiO_2 thin films for efficient energy harvesting, *J. Alloys Compd.*, 790, 1001–1013.

[8] Tahir, M.B., Hajra, S., Rizwan, M., and Rafique, M., 2017, Optical, microstructural and electrical studies on sol gel derived TiO_2 thin films, *Indian J. Pure Appl. Phys.*, 55 (1), 81–85.

[9] Fazli, F.I.M., Ahmad, M.K., Soon, C.F., Nafarizal, N., Suriani A.B., Mohamed, A., Mamat, M.H., Malek, M.F., Shimomura, M., and Murakami, K., 2017, Dye-sensitized solar cell using pure anatase TiO_2 annealed at different temperatures, *Optik*, 140, 1063–1068.

[10] Lin, C.P., Chen, H., Nakaruk, A., Koshy, P., and Sorrell, C.C., 2013, Effect of annealing temperature on the photocatalytic activity of TiO_2 thin films, *Energy Procedia*, 34, 627–636.

[11] Manickam, K., Muthusamy, V., Manickam, S., Senthil, T.S., Periyasamy, G., and Shanmugam, S., 2019, Effect of annealing temperature on structural, morphological and optical properties of nanocrystalline TiO_2 thin films synthesized by sol–gel dip coating method, *Mater. Today: Proc.*, 23 (1), 68–72.

[12] Nadzirah, S., Hashim, U., Kashif, M., and Shamsuddin, S.A., 2017, Stable electrical, morphological and optical properties of titanium dioxide nanoparticles affected by annealing temperature, *Microsyst. Technol.*, 23 (6), 1743–1750.

[13] Malek, M.F., Mamat, M.H., Musa, M.Z., Soga, T., Rahman, S.A., Alrokayan, S.A.H., Khan, H.A., and Rusop, M., 2015, Metamorphosis of strain/stress on optical band gap energy of ZAO thin films via manipulation of thermal annealing process, *J. Lumin.*, 160, 165–175.

[14] Malevu, T.D., Mwankemwa, B.S., Motloung, S.V., Tshabalala, K.G., and Ocaya, R.O., 2019, Effect of

annealing temperature on nano-crystalline TiO_2 for solar cell applications, *Physica E*, 106, 127–132.

[15] Mizuki, T., Matsuda, J.S., Nakamura, Y., Takagi, J., and Yoshida, T., 2004, Large domains of continuous grain silicon on glass substrate for high-performance TFTs, *IEEE Trans. Electron Devices*, 51 (2), 204–211.

[16] Achoi, M.F., Mamat, M.H., Zabidi, M.M., Abdullah, S., and Mahmood, M.R., 2012, Synthesis of TiO_2 nanowires via hydrothermal method, *Jpn. J. Appl. Phys.*, 51, 06FG08.

[17] Liu, M., Qiu, X., Hashimoto, K., and Miyauchi, M., 2014, Cu(II) nanocluster-grafted, Nb-doped TiO_2 as an efficient visible-light-sensitive photocatalyst based on energy-level matching between surface and bulk states, *J. Mater. Chem. A*, 2 (33), 13571–13579.

[18] Singh, S., Sharma, V., and Sachdev, K., 2017, Investigation of effect of doping concentration in Nb-doped TiO_2 thin films for TCO applications, *J. Mater. Sci.*, 52 (19), 11580–11591.

[19] Safiay, M., Nadzirah, S., Khusaimi, Z., Asib, N.A.M., Hamzah, F., and Rusop, M., 2017, Transmissivity property of nanostructured TiO_2 thin films, *International Conference on Engineering Technology and Technopreneurship (ICE2T)*, 18–20 September 2017, Kuala Lumpur, Malaysia.

[20] Mamat, M.H., Sahdan, M.Z., Khusaimi, Z., Ahmed, A.Z., Abdullah, S., and Rusop, M., 2010, Influence of doping concentrations on the aluminum doped zinc oxide thin films properties for ultraviolet photoconductive sensor applications, *Opt. Mater.*, 32 (6), 696–699.

[21] Ismail, A.S., Mamat, M.H., Md. Sin, N.D., Malek, M.F., Zoolfakar, A.S., Suriani, A.B., Mohamed, A., Ahmad, M.K., and Rusop, M., 2016, Fabrication of hierarchical Sn-doped ZnO nanorod arrays through sonicated sol–gel immersion for room temperature, resistive-type humidity sensor applications, *Ceram. Int.*, 42 (8), 9785–9795.